

RADIO-LOUD AGNS: THE X-RAY PERSPECTIVE

Rita M. Sambruna and Michael Eracleous

Pennsylvania State University, Dept. of Astron. & Astrophys., 525 Davey Lab, University Park 16802 (emails: rms@astro.psu.edu, mce@astro.psu.edu)

ABSTRACT

The X-ray emission of radio-loud (RL) AGNs is a powerful tool for probing the structure of the accretion flow in these objects. We review recent spectral and variability studies of RL AGNs, which show that these systems have systematically different X-ray properties than their radio-quiet (RQ) counterparts. Specifically, RL AGNs have weaker and narrower Fe K α lines and weaker Compton reflection components above 10 keV. The nuclear continuum of RL AGNs in the 2–10 keV band is well described by a power law with photon indices ~ 1.8 , similar to RQ AGNs of comparable X-ray luminosity. RL AGNs have little or no flux variability on short time scales ($\lesssim 0.5$ days); however, flux and spectral variations are observed on time scales of weeks in two well-monitored objects, 3C 390.3 and 3C 120. These properties strongly suggest that the central engines of the two AGNs classes are different. We discuss the implications of these observational results, in particular the possibility that the central engines of RL AGNs harbor an ion torus (also known as an Advection-Dominated Accretion Flow or ADAF). We show that a beamed component from the jet is unlikely in the majority of sources. Moreover, the X-ray data provide evidence that the circumnuclear environs of RL and RQ AGNs also differ: large amounts of cold gas are detected in BLRGs and QSRs, contrary to Seyfert galaxies of similar X-ray luminosity where an ionized absorber seems to be the norm. The role of future X-ray missions in advancing our understanding of the central engines of RL AGNs is briefly highlighted.

KEYWORDS: Radiogalaxies; X-rays; black hole; AGNs

1. THE X-RAY ADVANTAGE

The spectra and variability properties of AGNs are a diagnostic of the conditions of the matter in the inner parts of the accretion flow. Recent studies of X-ray-bright, radio-quiet (RQ) Seyfert galaxies have provided evidence that their X-ray emission is complex. At high energies, the most prominent features are the Fe K α emission line between 6 and 7 keV and the Compton reflection hump at $\lesssim 10$ keV, originating from a cold reprocessor near the central black hole. At soft X-rays, many Seyferts exhibit absorption from partially ionized gas with column densities $N_{\text{W}} \sim 10^{21}\text{--}10^{24}$ cm $^{-2}$ along the line of sight. The rapid flux variations of Seyfert galaxies on timescales of hours and even minutes (e.g., Edelson 2000) indicate that the X-ray source is compact and located very close to the central black hole.

In contrast, the X-ray spectra and variability of radio-loud (RL) AGNs¹ are not as well known. Past X-ray studies with *Einstein*, *EXOSAT* and *GINGA* showed that RL AGNs had systematically harder (i.e, flatter) X-ray continua than their radio-quiet counterparts (Wilkes & Elvis 1987; Shastri et al. 1993; Lawson & Turner 1997). These studies, however, were plagued by the low sensitivity and resolution of the instruments, in addition to the heterogeneity of the samples.

Fundamental progress was recently achieved with the advent of *ASCA* and *RXTE* (for a review of the *BeppoSAX* results, see Grandi 2000). The wide-band coverage of these instruments, combined to their higher sensitivity and/or resolution compared to older instruments, enable us to disentangle the various spectral components and study flux and spectral variability. We started a program of systematic study of the X-ray properties of RL AGNs, with the ultimate goal of elucidating the structure of the accretion flow in these systems and comparing it to RQ AGNs. Here we review the results of our *ASCA* and *RXTE* surveys (Sambruna, Eracleous, & Mushotzky 1999; Eracleous, Sambruna, & Mushotzky 1999; also reporting references to previous works), and present new observations of selected objects.

2. THE *ASCA* AND *RXTE* DATABASES FOR RL AGNS

In the following we concentrate on AGNs with lobe-dominated radio morphologies, which we define as those objects with either a 5 GHz radio power of $P_{5\text{ GHz}} > 10^{25} \text{ W Hz}^{-1}$ or with rest-frame 5 GHz-to-4400 Å flux-density ratios of $\mathcal{R}_{\text{rto}} > 10$, following Kellermann et al. (1994). There are 39 objects in the *ASCA* archive up to September 1998 which satisfy these criteria, of which 9 are Broad Line Radio Galaxies (BLRGs), 6 are Quasars (QSRs), 12 are Narrow Line Radio Galaxies (NLRGs), and 11 are Radio Galaxies (RGs). This subdivision depends on their optical spectral properties, namely, the presence of broad, permitted lines in their optical spectra and the luminosity of the [O III] $\lambda 5007$ line. Clearly the sample is not statistical or complete, and most likely is biased toward the brightest sources of each type.

Because of its high background rate, only the brightest sources, typically BLRGs, were observed by *RXTE*. Our sample (Eracleous et al. 1999) includes four BLRGs, namely 3C 120, 3C 111, 3C 382, and Pictor A, observed for typically ~ 40 ks during AO1 and AO2. These have fluxes $F_{2-10 \text{ keV}} \sim 1 - 4 \times 10^{-11} \text{ erg cm}^{-2} \text{ s}^{-1}$, ensuring that their spectra could be measured adequately with both the PCA and HEXTE. The NLRG Centaurus A was also observed with *RXTE*; the results are presented by Rothschild et al. (1999).

The BLRGs 3C 390.3 and 3C 120 were intensively monitored with *RXTE* in 1997 May and January for 134 and 150 ks, respectively (P.I.: R. Remillard), as part of multiwavelength campaigns. Here we present the preliminary results of our analysis of the archival data. We also discuss simultaneous *ASCA* 100 ks and *RXTE* 60 ks observations of 3C 382 obtained by us in 1999 March.

¹Here we will exclude blazars, as their continuum is entirely dominated by the the beamed jet emission.

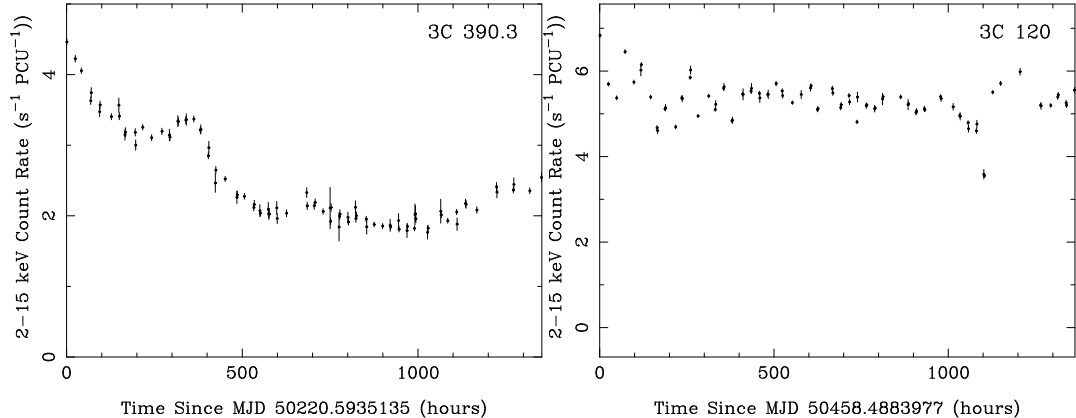


FIGURE 1. Light curves from *RXTE* monitoring observations of the BLRGs 3C 390.3 and 3C 120 in 1997 May and 1997 January, respectively. The light curves are binned at 4600 s. Flux variability is apparent, with different behaviors for the two sources. While 3C 390.3 shows a long-term trend, with large-amplitude variations on timescales of $\lesssim 2$ weeks, “flickering” variations are observed for 3C 120.

3. THE NUCLEAR X-RAY EMISSION OF RL AGNS

3.1. Continuum Shape

In the *ASCA* sample, a power law component is detected in 100% of BLRGs and QSRs and in 90% of NLRGs and RGs above 2 keV. The average photon index is $\langle \Gamma_{2-10 \text{ keV}} \rangle \sim 1.7 - 1.9$ for all the four subclasses, in agreement with unification models, which postulate that both type-1 and type-2 AGNs sport the same type of central engine, although view from a different direction. Indeed, in NLRGs and RGs the nuclear power law spectrum is heavily absorbed. The column densities detected by *ASCA* are $N_{\text{H}} \sim 10^{21-24} \text{ cm}^{-2}$ and are most likely due to the putative obscuring torus on parsec-scales (e.g., Urry & Padovani 1995). More surprising is the detection of similar columns of *cold* gas in a fraction of BLRGs and QSRs, which we discuss further below.

We compared the photon index distributions of the RL objects of our sample to those of RQ AGNs of matching X-ray luminosity, and found that the distributions of X-ray continuum slopes for the two classes are not demonstrably different. This finding is consistent with previous results that a flat X-ray component in RL AGNs is due to the beamed contribution of the jet (see above). This conclusion is bolstered by the fact that no correlation is found between the nuclear X-ray and core radio luminosities. This was expected since the AGNs in our sample are associated with lobe-dominated radio sources.

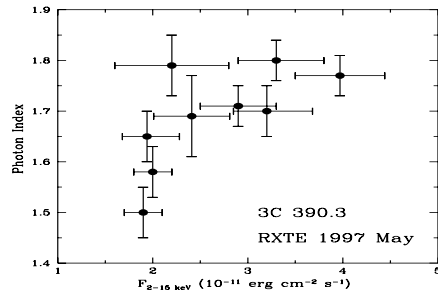


FIGURE 2. Spectral variability of 3C 390.3 during the *RXTE* intensive monitoring in 1997 May (see Figure 1). The photon index from fits to time-resolved *RXTE* spectra is plotted versus the observed flux. There is a trend of steeper slopes for increasing flux, and a large and probably intrinsic dispersion in spectral indices at lower fluxes.

3.2. Continuum Flux and Spectral Variability

While X-ray variability on short-timescales (from hours to minutes) is common in Seyfert 1s (e.g., Edelson 2000), no pronounced flux variations are observed in the BLRGs and QSRs of our *ASCA* and *RXTE* samples on timescales < 10 hours. The only exception is 3C 120, where flux changes with amplitude $\sim 20\%$ are present in the archival *ASCA* 40 ks observation. The lack of pronounced variability may be a consequence of the high luminosity of these objects since Seyferts of comparable luminosities have similar variability properties.

In contrast, significant X-ray flux and spectral variations on longer timescales are observed in two well-monitored BLRGs, 3C 390.3 and 3C 120. Figure 1 shows the *RXTE* 2–15 keV light curves obtained during the intensive monitorings in 1996 May and 1997 January, with a sampling characterized by short pointings roughly once a day for 60 days. Flux variability is readily apparent in both cases, with qualitatively different behaviors. 3C 390.3 exhibits a trend of decreasing flux by a factor 2 in ~ 20 days, with smaller changes (\sim a few percent) on timescales of $\lesssim 4$ days superposed. Non-linear variability was found in the soft X-ray light curve of this object from previous *ROSAT HRI* observations (Leighly & O’Brien 1998). In contrast, 3C 120 exhibits more erratic flux variations similar to “flickering”, with small-amplitude intra-day flares superposed on a constant baseline.

We investigated accompanying spectral variability by integrating PCA spectra during selected intervals in the light curves in Figure 1 corresponding to high, intermediate, and low states. We fitted the spectra in 4–20 keV with a model consisting of a power law, absorbed by the Galactic absorbing column, plus the Fe K α line at 6.4 keV. This model was chosen because it describes well the average PCA+HEXTE spectrum. Figure 2 shows the plot of the best-fitting photon index versus the 2–10 keV flux in the case of 3C 390.3. Spectral variability is readily apparent, with the

spectrum becoming steeper as the flux increases. Note, however, the large dispersion of slopes at low flux levels ($\lesssim 3 \times 10^{-11}$ erg cm $^{-2}$ s $^{-1}$), which is larger than the typical error bar, indicating a true intrinsic dispersion of values. A similar correlation between the X-ray slope and flux was previously observed in 3C 120 (Halpern 1985) and is consistent with the general trend of steeper-when-brighter observed in Seyfert 1s (Grandi et al. 1992).

3.3. The Fe K α Line

At high energies, the Fe K α line is detected with *ASCA* in 67% of BLRGs, 20% of QSRs, 33% of NLRGs, and 30% of RGs. It is generally broad in type-1 sources, with FWHM $\lesssim 50,000$ km s $^{-1}$ s, and unresolved in NLRGs and RGs. However, in most cases it is difficult to study the line profile due to the limited sensitivity of *ASCA* and the fact the line is weak in RL AGNs. More stringent constraints are provided by *RXTE* thanks to its larger collecting area. The Fe K α line is detected in the BLRGs of the *RXTE* sample with an Equivalent Width of EW $\lesssim 100$ eV, lower than what was measured by *ASCA* in most Seyferts (Figure 3a). Unfortunately, because of the poor *RXTE* resolution, the lines are unresolved, with FWHM $\lesssim 50,000$ km s $^{-1}$ at 90% confidence.

3C 390.3. Interesting constraints on the Fe K α line profile are obtained for the nearby, bright BLRG 3C 390.3. The Fe K α line profile is better fitted by a disk-line model than by a Gaussian model, with EW= 132_{-48}^{+40} eV; however, the inner disk radius is not constrained. A deep (134 ks) *RXTE* observation shows that the line is unresolved, with width FWHM $\lesssim 24,000$ km s $^{-1}$ (Figure 3c). These findings lend support to the idea that the Fe K α line in RL AGNs comes from the cold, thin accretion disk exterior to an ADAF. No reflection component is required to fit the *RXTE* data above 10 keV, with an upper limit to the covering factor $\Omega/2\pi \lesssim 0.5$ at 90% confidence.

3C 382. We observed 3C 382 simultaneously with *ASCA* and *RXTE* for 100 ks and 60 ks, respectively, in 1999 March, in order to study in detail the profile of the Fe K α line. This source was selected because it showed an extremely broad (FWHM $\sim 170,000$ km s $^{-1}$) line in a 40 ks *ASCA* exposure. The combination of spectra from this these two instruments lends itself to studying the line profile because it provides wide-band coverage and good resolution and collecting area in the energy range 6–7 keV. Thus it allows a reliable determination of the continuum underlying the emission line.¹

The 0.6–50 keV continuum is well described by a power law with photon index $\Gamma = 1.8 - 1.9$ and observed flux $F_{2-10 \text{ keV}} \sim 5 - 6 \times 10^{-11}$ erg cm $^{-2}$ s $^{-1}$, plus a bremsstrahlung plasma component with $kT \sim 0.4$ keV below 1 keV. The power law flux is a factor of ~ 2 higher than during the previous *ASCA* and *RXTE*

¹Unfortunately, it was later discovered that there are calibration discrepancies between the two instruments, which hamper the determination of the continuum. In practice, during the joint *ASCA+RXTE* fits the slope and normalization of the *ASCA* and *RXTE* continua were left untied.

observations. The simultaneous *ASCA* and *RXTE* observations confirm that the Fe $K\alpha$ line is quite broad compared to other BLRGs: we measure a width of FWHM $78,000_{-25,000}^{+31,000}$ km s⁻¹ at 90% confidence, and with $EW=228_{81}^{+131}$ eV, resolved at > 99% confidence. No improvement to the fit is obtained when a disk-line profile is used, nor when the reflection component is added. The upper limit to the solid angle subtended by any medium producing Compton reflection $\Omega/2\pi \lesssim 0.5$ at 90% confidence.

The large width of the Fe $K\alpha$ line in 3C 382 is puzzling and requires explanation. If the line is indeed as broad as we have measured it to be, this source stands out as the only BLRG with a Seyfert-like Fe $K\alpha$ line profile. Alternatively, the line could be a blend of different components originating in various parts of the accretion flow and/or the jet. We tested this idea adding a narrow unresolved Gaussian to the fit to the *ASCA+RXTE* data; while the fit is not improved, the degraded SIS resolution at the time of these observations does not allow us to rule out the presence of multiple components to the Fe $K\alpha$ line in 3C 382. Thus, the final solution to this puzzle will have to await observations at higher spectra resolution than *ASCA* can currently deliver.

3.4. The Reflection Component

The wide energy range (2–250 keV) covered by the PCA and HEXTE instruments on *RXTE* is well suited to the study of the Compton reflection in RL AGNs at energies above 10 keV. The strength of this component is parameterized in terms of $R = \Omega/2\pi$, i.e., the fraction of solid angle subtended by the reprocessor to the illuminating source. We find that the reflection component is generally weak or undetected in the BLRGs observed with *RXTE*, with strengths $R \lesssim 0.4$ –0.5. This is much weaker than what is typically observed in Seyfert 1s (Figure 3b).

Interestingly, the spectrum of the NLRG Centaurus A, includes an unresolved Fe $K\alpha$ line and no reflection component (Rothschild et al. 1999), consistent with unification models.

4. POSSIBLE INTERPRETATIONS

In the currently accepted accretion scenario for RQ AGNs, X-ray emission is produced in a hot “corona” overlaying and illuminating a standard, Shakura-Sunyaev accretion disk (e.g., Haardt, Maraschi, & Ghisellini 1994). In this picture the reprocessor (disk) subtends a solid angle of $\Omega = 2\pi$ to the illuminating source, as observed by *Ginga* and *RXTE* in Seyfert galaxies. The Fe $K\alpha$ line is emitted within a few gravitational radii from the black hole (Fabian et al. 1989), and has a skewed profile with a broad red wing. Its equivalent width depends on the solid angle subtended by the disk to the X-ray source.

In BLRGs we observe weaker reflection components, indicating $\Omega \approx \pi$. From this perspective, one possible scenario is that the inner parts of the disk (below some transition radius) inflate under the pressure of the ions which are much hotter than

the electrons, thus forming an ion torus or ADAF. The ion torus responsible for the emitted continuum radiation from radio to IR via synchrotron, bremsstrahlung, and/or inverse Compton emission. The cold, thin disk exterior to the ADAF produces the reflection component and the Fe $K\alpha$ line; both of these features would be weaker than in Seyferts since the disk subtends a solid angle $\Omega \approx \pi$ to the X-ray source.

For an assumed black hole mass of $M = 10^8 M_\odot$, the lack of X-ray flux variability on timescales $\lesssim 0.4$ days constrains the light-crossing radius of the emitting region to be $\gtrsim 100 R_g$ (where $R_g \equiv GM/c^2$ is the gravitational radius, with M the mass of the black hole). This is consistent with the expected light-crossing size of an ADAF, which is somewhere between a few light-hours and a few light-days. The ADAF scenario can also accommodate X-ray slopes similar to Seyferts, depending on the transition radius between the inner ADAF and the disk.

An alternative scenario was proposed by Woźniak et al. (1998) on the basis of similar results to ours, obtained from non-simultaneous, archival *ASCA*, *CGRO/OSSE*, and *Ginga* data. In that scenario the central engines of BLRGs harbor a standard, geometrically thin disk but the bulk of the X-ray continuum is produced by the inner parts of a *mildly* relativistic jet. The X-rays from the jet are emitted in a cone that is wide enough to illuminate the obscuring torus but not wide enough to illuminate the accretion disk. Thus, these authors proposed that the Compton reflection component and the Fe $K\alpha$ line are originate in the obscuring torus (the former via Thomson scattering and the latter via fluorescence). However, our result that RL AGN have similar X-ray slopes to RQ AGNs argues against a beamed component in the X-rays. Moreover, the scenario suffers from the additional drawback that X-rays from the jet are unlikely to be beamed in a wide-angle cone: since jet Lorentz factors are thought to have values around 10, the opening angle of the beam should be less than 10° . Therefore, the obscuring torus will not be illuminated by this beam.

These scenarios can in principle be tested further by studying the profile of the Fe $K\alpha$ line in detail with instruments such as *XMM* and *Astro-E*. If the ADAF scenario is correct, the line will be double peaked with FWHM $\lesssim 20,000 \text{ km s}^{-1}$ (as indicated in the case of 3C 390.3), corresponding to an inner radius of a few hundred R_g or more. If the Fe $K\alpha$ line is produced in the obscuring torus, i.e., at a very large distance from the central black hole, then its profiles will be rather narrow (FWHM $\sim 300 \text{ km s}^{-1}$), and thus unresolved by the *XMM* detectors and possibly even unresolved by the *Astro-E* calorimeter. Finally, if the Fe $K\alpha$ lines of BLRGs have the same profiles as those of Seyfert 1 galaxies, then these will be easily measurable in high signal-to-noise ratio spectra obtained with *XMM*.

It has also been suggested (Blandford & Znajek 1977; Koide et al. 1999) that RL AGNs harbor more rapidly spinning black holes than RQ sources. While this mechanism would provide a ready explanation for the formation and collimation of the jets, its implications for the broad-band and X-ray properties of the two AGN classes are less clear. Nevertheless, it should be possible at least in principle

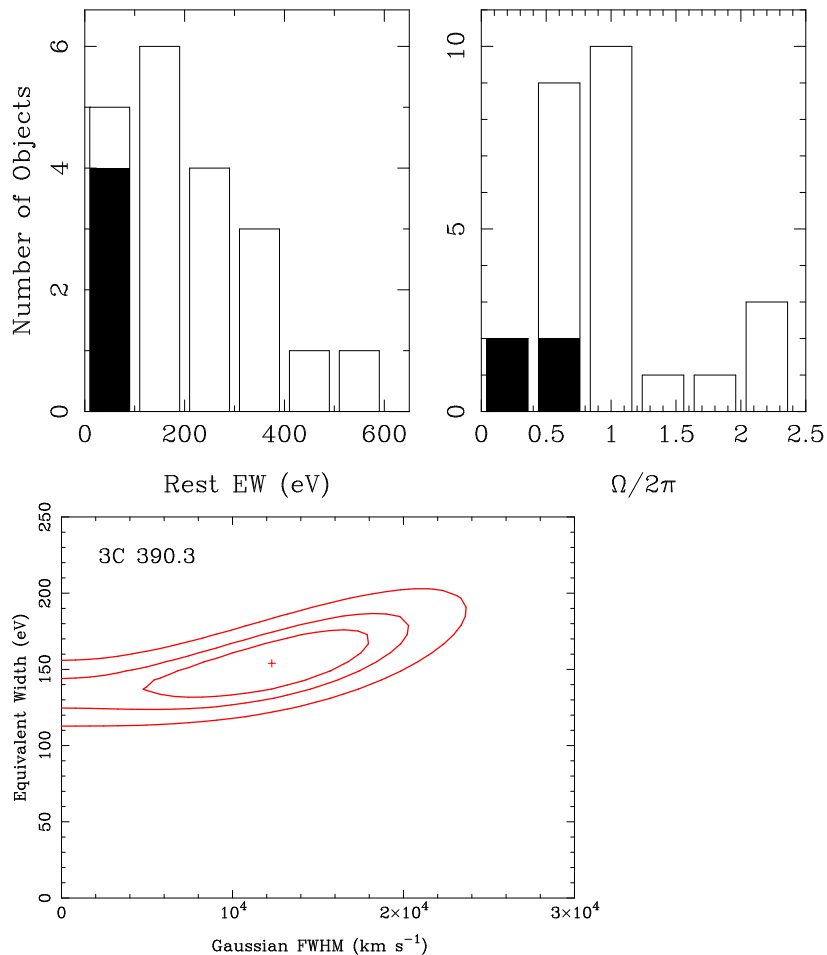


FIGURE 3. (a) *Left and (b) Center*: Histograms of the rest-frame EW of the Fe K α line and covering fraction of the reflection component, respectively, for the BLRGs of our *RXTE* survey (shaded) and for Seyfert 1s studied by *ASCA* and *GINGA* (open), from the literature (Nandra et al. 1997; Nandra & Pounds 1994). Radio-loud AGNs have weaker lines and Compton humps than radio-quiet AGNs. (c) *Right*: Contours at 68%, 90% and 99% confidence for the EW of the Fe K α line versus its velocity width from the fit to an archival 134 ks *RXTE* observation of 3C 390.3. The line is marginally resolved, with an interesting upper limit to its width of FWHM $\lesssim 24,000$ km s⁻¹.

to test this model through the shape of the Fe $K\alpha$ line (see Reynolds 2000 and references therein). This awaits the large collecting areas and resolutions of future X-ray missions, such as the proposed *Constellation-X* (NASA) and *XEUS* (ESA).

5. X-RAY ABSORPTION IN RL AGNS

X-ray observations of RL AGNs also provide constraints on the gas surrounding their central engines. While ionized absorption is common in Seyfert 1s (Reynolds 1997; George et al. 1998), no analogous evidence is found in the BLRGs of our sample, except in 3C 390.3. Instead, large columns of *cold* gas are detected in 50% of BLRGs and QSRs. In some case the absorbing columns are as high as those found in NLRGs and RGs. This is in contrast to unification models where the line of sight to type-1 sources should be devoid of cold material.

The columns detected in BLRGs and QSRs of our sample are similar to the columns observed in more distant RL QSRs with *ASCA* and *ROSAT* (Elvis et al. 1998; Cappi et al. 1997). This is apparent from Figure 4, where the excess X-ray column $N_{\text{H}^{\text{exc}}}$ (in the source's rest-frame) is plotted versus the nuclear 2–10 keV luminosity. While there is a large dispersion in the values of the column density at lower luminosity, no trends are present over more than five decades: the more distant sources have similar intrinsic absorbing columns to the nearby sources. Interestingly, while the BLRGs and QSRs of our sample are lobe-dominated, the more distant objects are core-dominated. This suggests that the absorber, common to both low- and high-redshift sources, must be isotropic in the sources' rest-frame, or subtend a relatively large solid angle to the central illuminating source. As discussed by Halpern (1997), the nature of the absorbing medium and its location relative to the emission line regions surrounding the central engine is unclear. It is plausible to place the X-ray absorber between the broad-line region and the central engine, as long as it does not contain a significant amount of dust. In this context the absorber could be a wind outflowing from the central engine (e.g., Blandford & Begelman 1999).

6. CONCLUSIONS

Recent observations at high sensitivity and resolution with *ASCA* and *RXTE* have shown that systematic differences in the X-ray properties of RL and RQ AGNs. The X-ray results suggest that the origin of the RL/RQ AGN dichotomy must be sought in the intrinsic properties of the central engines of these systems.

Much remains to be done to further our understanding of RL AGNs. The three major X-ray observatories of the next century, *Chandra*, *XMM*, and *Astro-E*, will have a central role as they will allow us to study in detail the Fe $K\alpha$ line profile, the nature of the mysterious X-ray absorber, and X-ray variability on the shortest timescales. Future X-ray observations at high sensitivity and spectral resolution will provide a giant leap forward in our understanding of RL AGNs (comparable to the one *ASCA* already provided for RQ AGNs), opening a new perspective on the origin

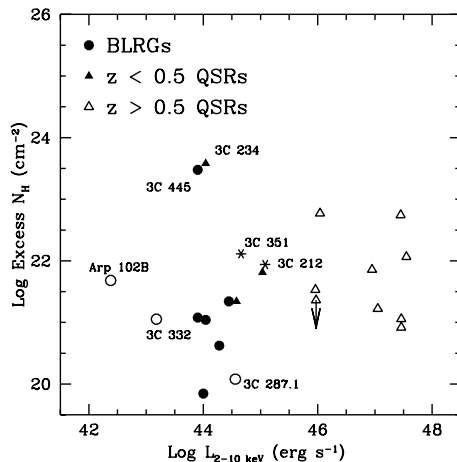


FIGURE 4. Plot of the intrinsic (rest-frame) excess N_{H} versus luminosity for the BLRGs and QSRs of our study, together with more distant sources studied with *ROSAT* and *ASCA* in the literature. No trends of the column density with luminosity are apparent over more than five decades.

of the RL/RQ AGN dichotomy.

ACKNOWLEDGEMENTS

We acknowledge support from NASA contract NAS-38252 and NASA grants NAG5-7733 and NAG5-8369.

REFERENCES

- ??landford, R. D. & Znajek, R. L. 1977, *MNRAS*, 179, 433
 ??landford, R.D. & Begelman, M. C. 1999, *MNRAS*, 303, L1
 ??appi, M. et al. 1997, *ApJ*, 478, 492
 ??delson, R. 2000, these proceedings
 ??lvis, M. et al. 1998, *ApJ*, 492, 91
 ??racleous, M., Sambruna, R. M., & Mushotzky, R. F. 1999, *ApJ*, submitted
 ??racleous, M. & Halpern, J. P. 1994, *ApJS*, 90, 1
 ??abian, A. C. et al. 1989, *MNRAS*, 238, 729
 ??eorge, I. M. et al. 1998, *ApJS*, 114, 73
 ??randi, P. 2000, these proceedings
 ??randi, P. et al. 1992, *ApJS*, 82, 93
 ??aardt, F., Maraschi, L., & Ghisellini, G. 1994, *ApJ*, 432, L95
 ??alpern J. P. 1985, *ApJ*, 290, 130

- ??alpern, J. P. 1997, in “Mass Ejection from AGNs”, ASP Conference Series, No. 128 (San Francisco: ASP), 41
- ??ellerman, K. et al. 1994, AJ, 108, 1163
- ??oide, S., Shibata, K., & Kudoh, T. 1999, ApJ, 522, 727
- ??awson, A. J. & Turner, M. J. L. 1997, MNRAS, 288, 920
- ??eighly, K.M. & O’Brien, P. T. 1997, ApJ, 481, L15
- ??andra, K. et al. 1997, ApJ, 477, 602
- ??andra, K. & Pounds, K. A. 1994, MNRAS, 268, 405
- ??tak, A. et al. 1998, ApJ, 501, L37
- ??ees, M.J. et al. 1982, Nature, 295, 17
- ??eynolds, C. S. 1997, MNRAS, 286, 513
- ??eynolds, C. S. 2000, these proceedings
- ??othschild, R. et al. 1999, ApJ, 510, 651
- ??ambruna, R. M., Eracleous, M., & Mushotzky, R. F. 1999, ApJ, in press (astro-ph/9905365)
- ??hastri, P., et al. 1993, ApJ, 410, 29
- ??rry, C. M. & Padovani, P. 1995, PASP, 107, 803
- ??ilkes, B. J. & Elvis, M. 1987, ApJ, 323, 293
- ??oźniak, P. et al. 1998, MNRAS, 299, 449